Molecular Therapy
Methods & Clinical Development
Original Article

Genome editing using *Staphylococcus aureus* Cas9 in a canine model of glycogen storage disease Ia

Benjamin Arnson,[1,2,6] Hye Ri Kang,[3,6] Elizabeth D. Brooks,[1] Dorothy Gheorghiu,[1] Ekaterina Ilich,[1] David Courtney,[4] Jeffrey I. Everitt,[5] Bryan R. Cullen,[2] and Dwight D. Koeberl[1,2]

[1]Division of Medical Genetics, Department of Pediatrics, Duke University Medical School, Durham, NC, USA; [2]Department of Molecular Genetics & Microbiology, Duke University Medical Center, Durham, NC, USA; [3]Department of Pediatrics, UT Southwestern Medical Center, Dallas, TX, USA; [4]Wellcome-Wolfson Institute for Experimental Medicine, Queen's University Belfast, Belfast, UK; [5]Department of Pathology, Duke University School of Medicine, Durham, NC, USA

Glycogen storage disease type Ia (GSD Ia) is the inherited deficiency of glucose-6-phosphatase (G6Pase), associated with life-threatening hypoglycemia and long-term complications, including hepatocellular carcinoma formation. Gene replacement therapy fails to stably reverse G6Pase deficiency. We attempted genome editing using two adeno-associated virus vectors, one that expressed *Staphylococcus aureus* Cas9 protein and a second containing a donor transgene encoding G6Pase, in a dog model for GSD Ia. We demonstrated donor transgene integration in the liver of three adult-treated dogs accompanied by stable G6Pase expression and correction of hypoglycemia during fasting. Two puppies with GSD Ia were treated by genome editing that achieved donor transgene integration in the liver. Integration frequency ranged from 0.5% to 1% for all dogs. In adult-treated dogs, anti-SaCas9 antibodies were detected before genome editing, reflecting prior exposure to *S. aureus*. Nuclease activity was low, as reflected by a low percentage of indel formation at the predicted site of SaCas9 cutting that indicated double-stranded breaks followed by non-homologous end-joining. Thus, genome editing can integrate a therapeutic transgene in the liver of a large animal model, either early or later in life, and further development is warranted to provide a more stable treatment for GSD Ia.

INTRODUCTION

Glycogen storage disease type Ia (GSD Ia) is the inherited deficiency of glucose-6-phosphatase (G6Pase) caused by pathogenic mutations in the *G6PC* gene. GSD Ia is associated with life-threatening hypoglycemia, as well as longer term adverse effects including hepatocellular adenoma (HCA) and hepatocellular carcinoma (HCC).[1,2] While dietary therapy with uncooked cornstarch has succeeded in prolonging the lifespan of people with this condition, it fails to reliably prevent long-term complications of GSD Ia, including short stature, progressive renal failure, HCA, and, less frequently, HCC. The liver and kidney involvement has been attributed to accumulations of glycogen and lipids in these tissues that persists despite dietary therapy. Treatments for HCA and HCC have included resection or liver transplantation, and transplantation corrected the biochemical abnormalities associated with GSD Ia, including hypoglycemia and hyperlipidemia.[1,2] The efficacy of liver transplantation suggested that liver-targeted gene therapy could be efficacious, both by preventing tumor formation and clinical symptoms related to hypoglycemia. We and others have successfully piloted adeno-associated virus (AAV) vectors that delivered a *G6PC* transgene to correct G6Pase deficiency. However, the duration of the effect was limited, as hepatic AAV vector genome abundance decreased rapidly. followed by a more gradual loss of biochemical correction.[3–5] Approaches to this problem have included higher vector dosages[6,7] and the re-administration of the vector before the formation of anti-AAV antibodies.[8] These approaches have not comprehensively addressed the loss of efficacy due to the loss of AAV vector genomes in animal models for genetic disease. For example, a recent study in neonatal *G6pc*$^{-/-}$ mice revealed that, despite the correction of G6Pase deficiency by AAV vector-mediated gene therapy, autophagy was only partially restored in the liver.[9]

Genome editing has been initiated to correct a mutation or integrate a transgene as a method to stably treat liver metabolic diseases, including GSD Ia.[10,11] An initial genome editing study in GSD Ia mice used a zinc finger nuclease (ZFN)-mediated genome editing method.[10] More recently, a Cas9-mediated editing strategy corrected a point mutation underlying GSD Ia in a mouse model by introducing donor DNA template via homology directed repair (HDR).[12] Genome editing with Cas9 uses a single guide RNA (sgRNA) to target an endonuclease, Cas9, to DNA and to cleave it, creating a double-stranded break that is repaired by either of two processes: (1) non-homologous end-joining (NHEJ) that is error prone and often results in short insertions or deletions (indels) at the cleavage site; or (2) HDR,

Received 11 April 2022; accepted 3 March 2023;
https://doi.org/10.1016/j.omtm.2023.03.001.

[6]These authors contributed equally

Correspondence: Dwight D. Koeberl, Box 103856, Duke University Medical Center, Durham, NC 27710, USA.
E-mail: dwight.koeberl@duke.edu

which uses a donor sequence with homology to both sites of the break to incorporate the donor sequence.[13] HDR is preferred as it can repair the break to the original sequence or incorporate the sequence from the donor template.[14,15]

Here, we report the development of a Cas9-mediated genome editing strategy in a canine model of GSD Ia that uses two AAV vectors to deliver the needed components. We have evaluated HDR *in vitro* and *in vivo*, demonstrating that transgene integration is feasible in a large animal model for GSD Ia.

RESULTS

Initially, genome editing was evaluated in cultured GSD Ia dog fibroblasts, which were transfected with plasmids containing the vector transgenes. One vector delivered the *S. aureus* Cas9 endonuclease (AAV-SaCas9) and an sgRNA expression cassette that directs SaCas9 to cleave the *G6PC* gene at exon 1/intron 1 boundary, while a second vector (AAV-cG6PC) delivered a repair template (donor) to induce HDR and to integrate a functional *G6PC* gene (Figure 1A). To avoid potential problems caused by the limited DNA packaging capacity of AAV, we chose to express the *S. aureus* Cas9 protein, rather than the more commonly used *Streptococcus pyogenes* Cas9 protein. The *S. aureus* Cas9 open reading frame (ORF) is, at 3162 base pairs (bp) in length, substantially smaller than the 4107-bp *S. pyogenes* Cas9 ORF, yet *S. aureus* Cas9 shows a similar level of genome editing activity in mammalian cells.[16] The two vector plasmids were functional, as demonstrated by the generation of indels detected in the Surveyor assay (Figure 1B) and transgene integration in canine GSD Ia fibroblasts (Figure 1C). Integration depended on the presence of CRISPR-Cas9, because transfection with donor alone resulted in no detectable integration events. Sequencing of transgene integration events confirmed its location in the dog *G6PC* exon 1/intron 1 boundary in the genome (Figure 1D).

Three adult dogs were treated with two AAV-based vectors expressing SaCas9 and an sgRNA, or expressing a G6Pase transgene, at 34 months of age at relatively high vector dosages (1×10^{13} vg/kg for AAV7-cG6PC and 2×10^{12} vg/kg for AAV7-SaCas9) (Figure 2A). All three dogs had a liver biopsy 2 months before treatment with editing vectors and 4 and 16 months after receiving vector. The dogs had previously received three prior treatments with gene replacement using other AAV serotypes between birth and age 3 months (Table S1) and with a brief course of rapamycin.[17] Transgene integration was detected in all three dogs' liver biopsies at months 4 and 16 after administration of the editing vectors (Figure 2B). The editing vector genomes, AAV-cG6PC and AAV-SaCas9, were detected at months 4 and 16, as was the original gene replacement vector genome, AAV-G6Pase (Figures 2C–2E). Evaluation of biochemical correction, in comparison with untreated GSD Ia dog liver, revealed significantly increased G6Pase in comparison with untreated dogs with GSD Ia (Figure 2F). At 32 months of age, the dogs had 29 ± 8% of normal G6Pase activity in liver, which increased to 43 ± 5% at 38 months of age, 4 months after receiving both donor and CRISPR vectors. However, the difference in G6Pase at 4 months was not statistically significant, in comparison with baseline (4 months vs before CRISPR vector administration [BC]) (Figure 2F). Liver G6Pase activity decreased to 32 ± 3% at 50 months of age, indicating that the majority of transgene expression was from episomal AAV vector genomes that were lost over the intervening 12 months. Liver glycogen content was significantly decreased in comparison with untreated dogs with GSD Ia (Figure 2G), and remained stably low after genome editing. However, there was no decrease in glycogen content following vector administration (4 months vs BC) (Figure 2G). Microscopic examination of liver biopsy samples revealed similar histopathological features in all three treated dogs both pre- and post-treatment with genome editing (Figure S1). However, these changes were markedly decreased in comparison with an untreated adult dog with GSD Ia, and were consistent with stable correction from *G6PC* transgene expression. Furthermore, genome editing was accompanied by correction of hypoglycemia during fasting, as demonstrated by stably increased blood glucose into the normal range of unaffected controls (Figure 2H). This group of puppies (later treated with genome editing) had normal blood glucose at 2 weeks of age after AAV vector administration (139 ± 13 mg/dL) after a 2-h fast. In contrast, untreated, affected puppies could not fast longer than 2 h and had low blood glucose (9 ± 9.5 mg/dL; age-matched normal range, 110 ± 23 mg/dL). This group of puppies had normal area under the curve (AUC) blood glucose during the 8-h fasting test at 2 weeks of age after gene therapy (701 ± 113 mg/dL; normal, 360–720 mg/dL). However, the AUC eventually decreased before genome editing, and normalized after the administration of genome-editing vectors (Figure 2H).

Antibody responses were evaluated to assess any effect from immune responses on genome editing. A puppy treated as a neonate with the editing vectors (described below) was included as a control. Anti-AAV7 IgG antibodies were positive after vector administration, demonstrating the expected response to AAV7 vector administration in all dogs (Figure 3A). In contrast with the situation for the neonatally treated dog that maintained low anti-SaCas9, anti-SaCas9 was positive for adult dogs treated with genome editing at baseline, and at months 4 and 16 after editing (Figure 3B), suggesting that adult dogs were exposed to *S. aureus* before receiving gene-editing vectors. Elevated transaminases, both alanine aminotransferase and aspartate aminotransferase, were variably elevated before and after genome editing (Figure S2), which were attributed to the liver effects of GSD Ia.[18]

Thereafter, two puppies with GSD Ia were treated with genome editing as neonates, dosing at $4–5 \times 10^{13}$ vg/kg for AAV7-cG6PC and with 5-fold lower amounts of AAV7-SaCas9 (Table S1). One puppy received two doses of gene replacement therapy at ages 2 and 3 months using two different AAV serotypes, while the second only received gene replacement therapy once at 2 months of age. Liver biopsies were taken at both 4 and 16 months after treatment with gene-editing vectors. The donor vector was efficacious based on the reversal of hypoglycemia and survival of GSD Ia puppies, given that affected puppies have previously demonstrated severe hypoglycemia

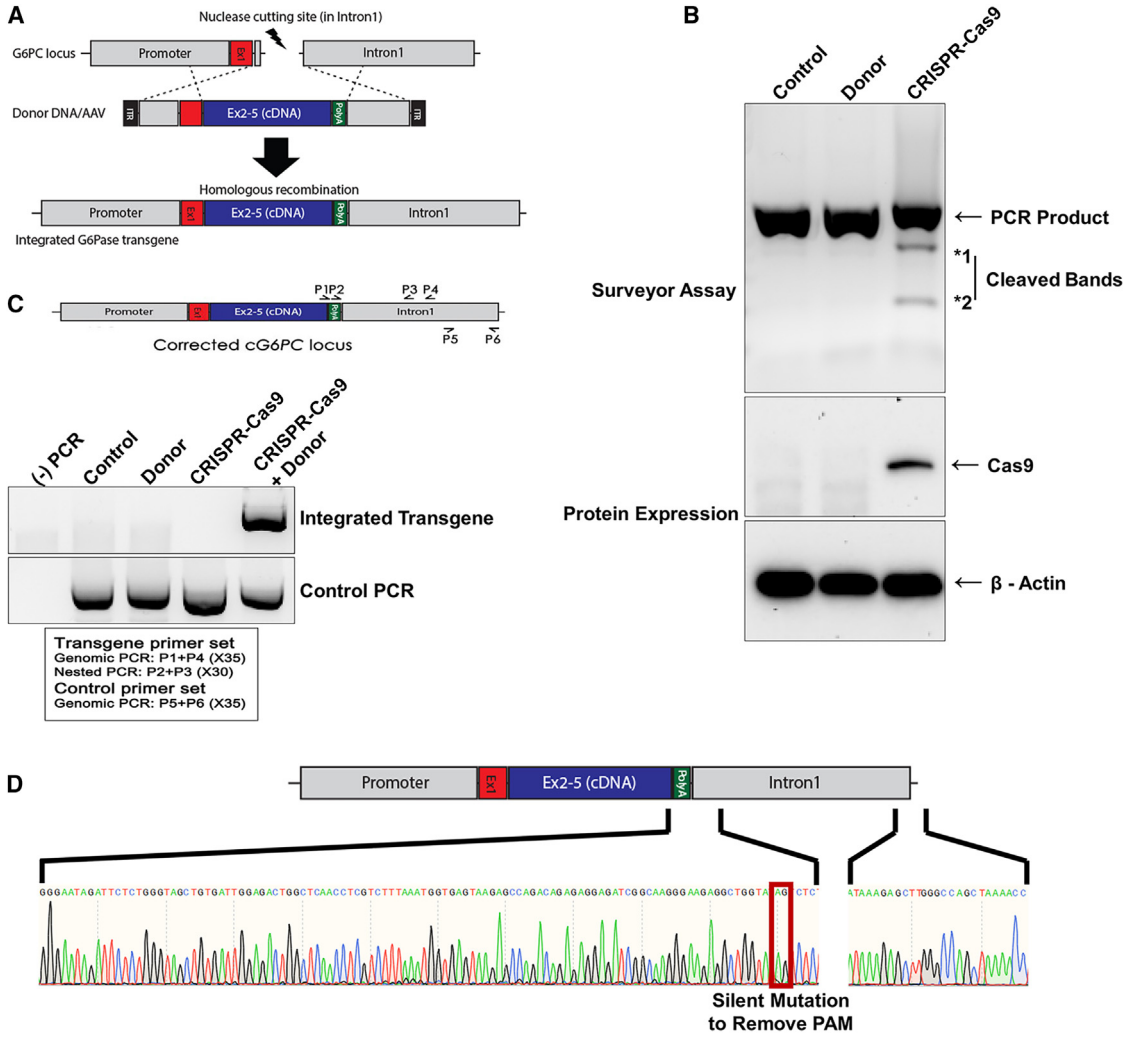

Figure 1. Transgene integration *in vitro*

(A) Schematic of CRISPR-Cas9 cutting at the exon 1/intron 1 boundary of the dog *G6PC* gene, followed by HDR to achieve integration of a canine *G6PC* cDNA downstream of the *G6PC* promoter. (B) Cultured dog skin fibroblasts were transfected with the pAAV-CRISPR-Cas9 plasmid, pAAV-cG6PC (donor) plasmid, or untransfected (control) and incubated for 72 h before DNA was extracted for the Surveyor assay. The Surveyor assay revealed the expected bands reflecting indels from NHEJ. Western blotting revealed a single band for Cas9 protein. (C) Dog fibroblasts were transfected with the CRISPR-Cas9 plasmid alone, donor plasmid alone, both CRISPR-Cas9 and donor plasmids, or untransfected (control). The integration PCR used primers P1 and P4 in an initial PCR, followed by P2 and P3 in a second, "nested" PCR. The integration PCR revealed the presence of the band expected from the junction between dog *G6PC* gene and vector transgene by HDR. (D) Sequencing of the integration PCR product confirmed the donor sequence was inserted in the dog *G6PC* gene at the exon 1/intron 1 boundary. Select sequence shows the transition from the polyA sequence to intron 1 containing a silent mutation that removes the PAM sequence. The transition from the end of the vector's right homology arm into the dog G6PC genomic sequence is also shown.

and very high mortality in the first 2 months of life when treated with diet therapy alone.[19] However, these CRISPR-Cas9-treated puppies subsequently developed recurrent hypoglycemia and were treated with gene replacement using a new AAV serotype following our established protocols,[20] which reversed their symptoms (Figure 4A). Integration of the donor transgene was detected in both puppies' liver biopsies at months 4 and 16 after administration of the editing vectors (Figure 4B). Both the editing vector genomes (AAV-cG6PC and AAV-SaCas9) and the gene replacement vector genome (AAV-G6Pase) were detected at months 4 and 16 (Figures 4C–4E). Evaluation of biochemical correction, in comparison with untreated GSD Ia dog liver, revealed increased G6Pase (Figure 4F) and decreased glycogen content (Figure 4G) that was stable. Furthermore, blood glucose during fasting decreased in the first months of life and stabilized thereafter near the normal lower limit (Figure 4H). Genome editing treated puppies had normal blood glucose at 2 weeks of age after

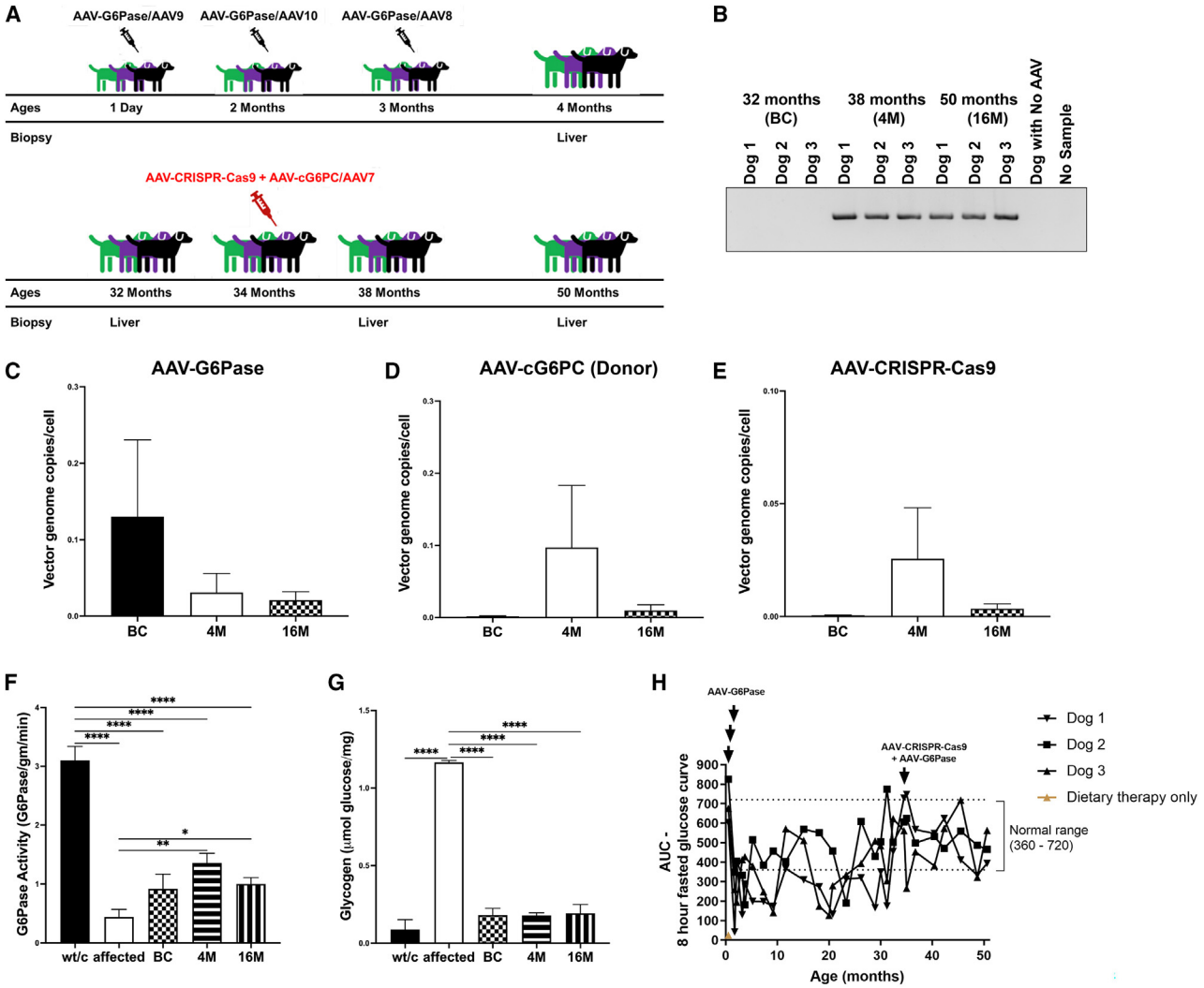

Figure 2. Dogs with GSD Ia treated initially with gene replacement followed by genome editing

(A) Puppies with GSD Ia were initially treated with AAV-G6Pase during infancy at the indicated ages, and later with genome editing including the AAV-CRISPR-Cas9 and AAV-cG6PC (donor) vectors at 34 months of age (see Table S2 for details). (B) Integration PCR revealed the presence of integrated donor at 38 months of age, or 4 months after administration of genome editing. In contrast, no integration was detected at 32 months of age, BC. (C) Vector genomes in liver were quantified with quantitative PCR, revealing low copy number (<0.01 vg/nucleus) at 4 months of age after gene replacement therapy (4M), and higher copy numbers for the (D) AAV-cG6PC and (E) AAV-CRISPR-Cas9 vectors 4 months after genome editing. The latter vectors trended toward greater copy number 4 months following genome editing ($p = 0.09$). (F) Liver G6Pase and (G) glycogen content were analyzed 4 and 16 months after genome editing at 34 months of age, and both assays reflected corrections of the biochemical abnormalities in comparison with untreated affected controls. Normal activity was measured in a group of three unaffected dogs (two carriers and one wild type; both genotypes are accepted as normal controls in published studies of animals with GSD Ia). (H) An 8-h fasting test revealed increased AUC for blood glucose obtained every 2 h for up to 8 h of fasting after genome editing, in comparison with baseline. The normal range for AUC is indicated by dotted lines. Mean ± standard deviation is shown in histograms. *=p<0.05, **=p<0.01, ***=p<0.001, ****=p<0.0001.

AAV vector administration (155 ± 28 mg/dL) after a 2-h fast, which was markedly higher than for untreated, affected puppies that had low blood glucose (9 ± 9.5 mg/dL; age-matched normal range, 110 ± 23 mg/dL). The genome-editing-treated puppies had a normal area AUC for blood glucose during the 8 h fasting test at 2 weeks of age (676 ± 95 mg/dL; normal, 360–720 mg/dL), which subsequently decreased to below the normal range, indicating the need for additional treatment (Figure 4H).

Integration of the therapeutic cG6PC transgene was quantified using a long-range nested polymerase chain reaction (PCR) and compared with a standard curve using a synthetic DNA template containing the transgene flanked by canine G6PC genomic DNA (Figures 5A–5C). All three dogs treated as adults contained the integrated transgene at months 4 and 16 (0.47% ± 0.19% and 0.51% ± 0.29%) with the transgene appearing to be stable (Figure 5D). Both dogs treated as infants also contained detectable transgene integrations that remained

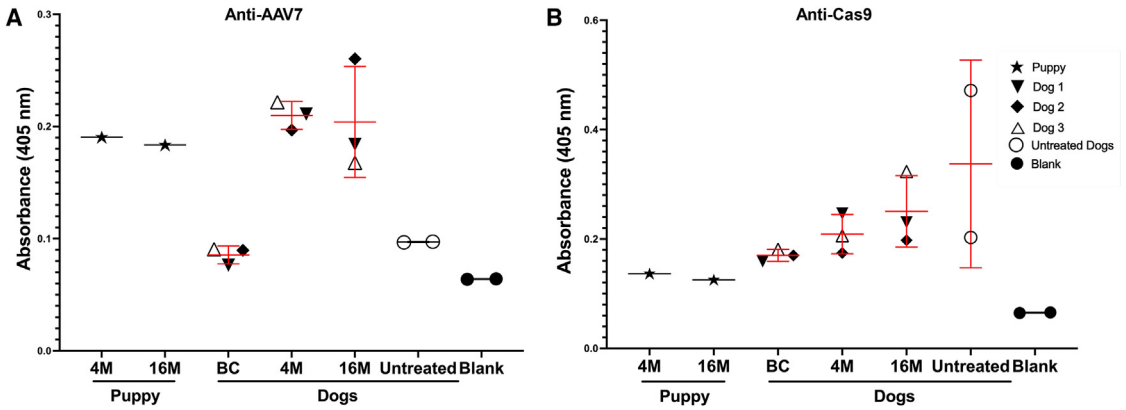

Figure 3. Monitoring for immune responses

(A) The IgG response determined by ELISA for anti-AAV7 and for (B) anti-SaCas9. A puppy treated with AAV-CRISPR-Cas9 and AAV-cG6PC (donor) vectors as a neonate was included as a positive control. Time following genome editing is indicated. Anti-AAV7 was similar to the untreated control before treatment, and increased after AAV7 vector administration. In contrast to the situation for the neonatally treated dog that remained negative, anti-SaCas9 was positive for dogs treated with genome editing at baseline and 4 months (4M) and 16 months (16M) later. Mean ± standard deviation is shown.

stable from months 4 to 16 (1.00% ± 0.13% and 0.95% ± 0.13%) (Figure 5E).

Expression of the integrated transgene was measured by next-generation sequencing of canine G6PC transcripts. Transcripts expressed from the integrated vector were detected by unique single nucleotide polymorphisms in the sequence and compared with the total cG6PC transcripts expressed, including those from the endogenous locus and episomal vectors. For the three dogs treated as adults, integrated transcripts were detected at months 4 and 16 (0.63% ± 0.61% and 0.60% ± 0.50%) (Figure 6A). The two dogs treated as infants also had detectable transcripts expressed from the integrated transgene at months 4 and 16 (0.44% ± 0.11% and 0.38% ± 0.14%) (Figure 6B). For all dogs, the transcript expression remains stable 16 months after treatment. CRISPR-Cas9 activity at the target site at the exon 1/intron 1 boundary in *G6PC* was evaluated by the Surveyor assay, which detected no detectable indel formation following vector administration that would indicate NHEJ at double-stranded breaks created by CRISPR-Cas9 (Figure S3). Indel formation was subsequently evaluated by next-generation amplicon sequencing to detect small indels generated at the locus, indicating DNA cleavage repaired by NHEJ instead of HDR after CRISPR-Cas9 administration. The three adult dogs had indel rates of 0.81% ± 0.78% and 0.80% ± 0.76% at months 4 and 16 (Figure 6C). One of the adult dogs had extremely low indel formation (<0.1% at months 4 and 16), indicating low nuclease activity and accounting for the wide variability. Both dogs treated as puppies had higher rates of indel formation at months 4 and 16 (3.13% ± 1.10% and 2.59% ± 0.73%) (Figure 6D). To assess specificity of the CRISPR-Cas9 vector, we analyzed the 10 most similar sites for potential off-target activity (Table 1). For nine sites, there was no significant increase in the rates of indel formation compared with an untreated dog control. Indel formation at the CCDC170 locus was increased 1.8- to 2.9-fold for the treated dogs compared with the untreated control dog.

DISCUSSION

The current study confirmed transgene integration with HDR using a CRISPR-Cas9-mediated genome editing strategy in the liver of dogs with GSD Ia that used a donor transgene containing *G6PC*, and a SaCas9 transgene and sgRNA in *trans*, which were delivered by two AAV vectors. Despite a low efficiency of transgene integration of only 0.5% to 1%, the donor vector expressed *G6PC* and demonstrated partial efficacy based upon the resolution of symptoms in neonatal puppies and the correction of hypoglycemia in older dogs after treatment. This experiment demonstrated genome editing in the liver of a large animal model for an inherited metabolic disorder using HDR to insert a therapeutic transgene, which is an important step toward the development of genome editing to treat genetic diseases in humans. HDR-mediated transgene integration was demonstrated after vector administration to newborn or adult dogs. Similar to human patients, adult dogs had evidence for a memory immune response to SaCas9 (Figure 3B), even before genome editing.[21] However, genome editing was possible in adult dogs despite the presence of anti-Cas9 immune responses. Furthermore, the strategy used has the advantage of treating all patients with GSD Ia, regardless of the underlying mutations, in contrast with genome editing targeted to a specific mutation.[12]

Genome editing has been extensively developed in mouse models for inherited disorders of the liver, similar to GSD Ia. In the first genome editing study for GSD Ia, we used ZFNs to cleave the *Rosa26* locus and enable integration of a G6PC-expressing transgene in mice.[10] More recently, Arnaoutova and colleagues developed CRISPR-Cas9 mediated cleavage of the *G6pc* locus followed by HDR of a donor DNA template to correct a pathogenic missense variant in GSD Ia and reported correction in 0.7% of alleles.[12] We currently demonstrated transgene integration in 0.5–1% of alleles in the canine model for GSD Ia (Figure 5). In other mouse models, AAV vectors were developed to allow insertion of a promoterless transgene in the *Alb* locus that was highly expressed from the endogenous *Alb* promotor. This

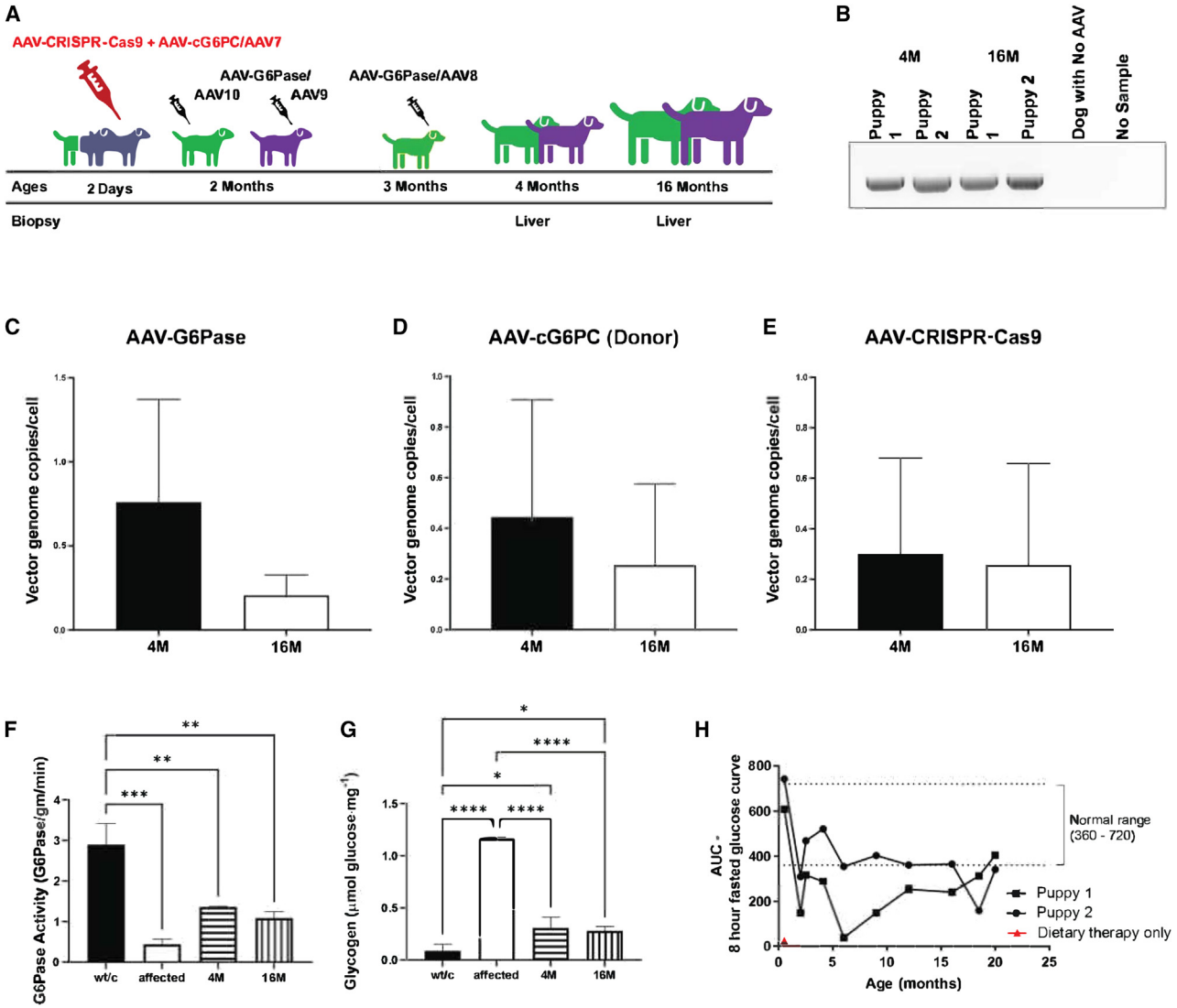

Figure 4. Puppies with GSD Ia treated initially with genome editing followed by gene therapy

(A) Puppies with GSD Ia were initially treated with AAV-CRISPR-Cas9 and AAV-cG6PC (donor) to perform neonatal genome editing at 2 days of age, followed by gene replacement therapy with one or more alternative serotypes of AAV to control symptoms of GSD Ia at the indicated ages for the individual puppies (puppy 1 shown in green, puppy 2 in purple, see Table S2 for details). The control group of dogs received 3 doses of gene replacement therapy during infancy (shown as dogs 1–3 in Table S1). (B) Integration PCR revealed the presence of integrated donor in two of three puppies 4 months (4M) after vector administration. (C–E) Vector genomes were quantified with quantitative PCR. (F) Liver G6Pase and (G) glycogen content were stable after genome editing at 2 days of age, although both assays reflected corrections of the biochemical abnormalities in comparison with untreated affected controls. (H) An 8-h fasting test revealed stable AUC for blood glucose obtained every 2 h up to 8 h fasting after a slight decrease after genome editing and gene replacement, in comparison with normal. The normal range for AUC is indicated by dotted lines. Mean ± standard deviation is shown in histograms. *=p<0.05, **=p<0.01, ***=p<0.001, ****=p<0.0001.

strategy has treated both Crigler-Najar disease and methylmalonic acidemia successfully.[22,23] Both groups saw editing rates of less than 1% in mice initially, but the integrated transgene correcting methylmalonic acidemia increased to nearly 20% of alleles by 11 months after editing. Another mouse study used dual AAV genome editing vectors to deliver CRISPR-Cas9 and a donor transgene, which corrected the pathogenic variant in phenylketonuria resulting in 0.96% of alleles edited in absence of an NHEJ inhibitor to increase HDR.[21,24] Last, a mouse model of tyrosinemia type I was treated with editing plasmids delivered via hydrodynamic tail vein injection and detected 9% editing efficiency, albeit in a model with strong positive selection for corrected hepatocytes.[25] In GSD Ia, the need for rapid transgene expression to prevent mortality[19] prompted the inclusion of homologous sequence from the *G6PC* promoter to both drive expression from the unintegrated vector and to integrate the transgene such that it will be expressed from the endogenous *G6PC*

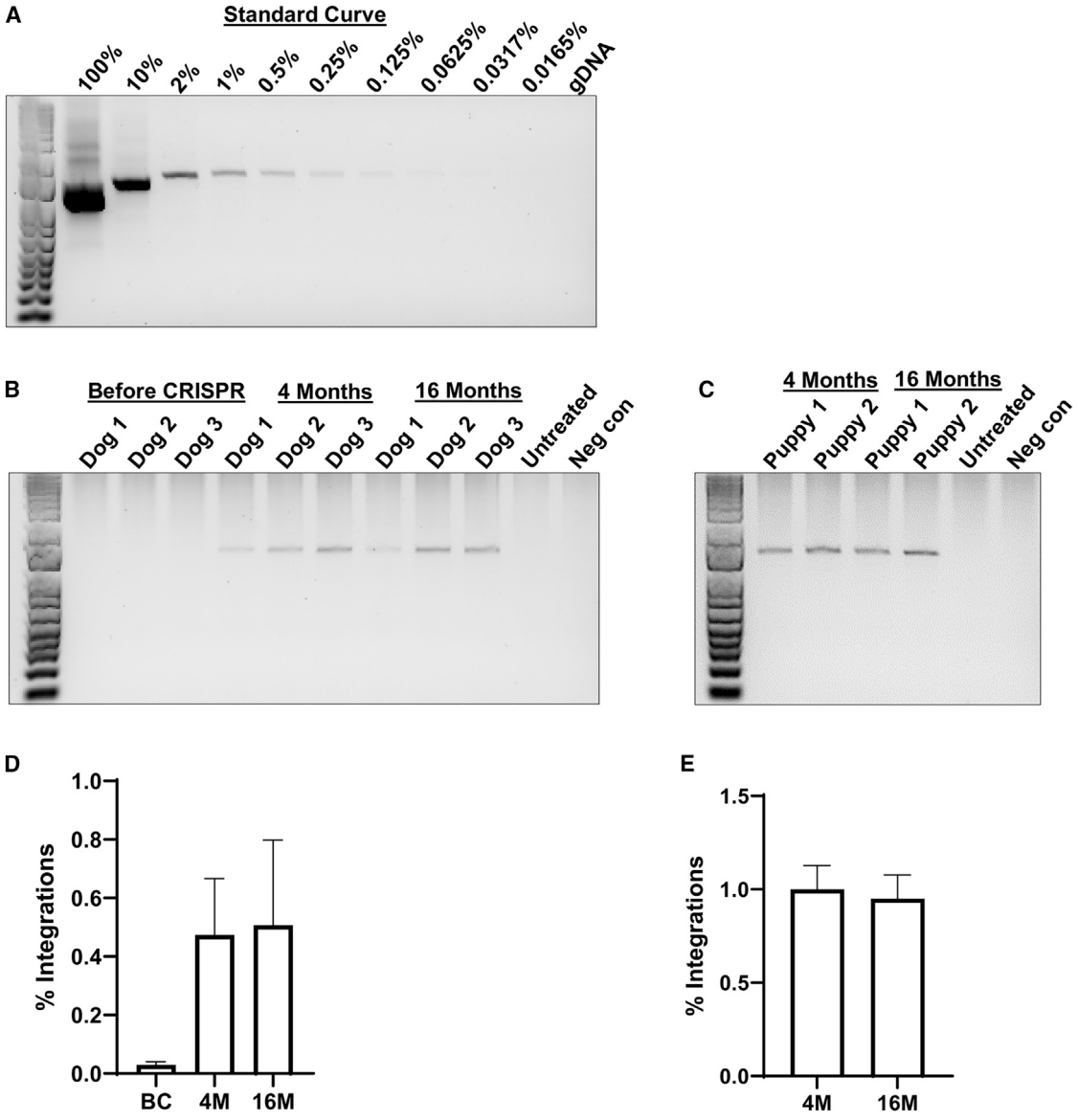

Figure 5. cG6PC transgene integration assay

(A) Long-range PCR was used to quantify integration of the cG6PC transgene (donor) at the G6PC locus in dogs. A standard curve was generated using serial dilutions of a starting template, which consisted of the purified junction fragment from integrated vector in intron 1 of *G6PC* that was generated by the integration PCR. The amount of starting template was calculated to represent 0.0165%–100% modification of intron 1. (B) Quantification of transgene integration in dogs treated with vectors as adults and (C) puppies. The relative intensities of the integration PCR products for liver DNA samples from dogs and puppies were compared with the standard curve to quantify the frequency of integration for each sample. (D) Dogs and (E) puppies receiving genome editing vectors had the indicated frequency of integrated transgene in the liver. Mean ± standard deviation is shown.

promoter (Figure 1A). This approach is optimized to treat GSD Ia, initially as a gene replacement therapy with the donor vector producing G6Pase, and later with the endogenous *G6PC* promoter driving regulated expression of G6Pase to avoid the risk for overexpression that would create prediabetes.[26]

In the adult dogs, G6Pase activity increased after administration of the editing vectors up to 43% of normal levels and glycogen content remained stable for up to 16 months. However, the majority of that liver G6Pase is attributable to transgene expression from episomal donor vector, given that the donor contains the canine *G6PC* promoter. Of note, the canine *G6PC* transgene included in the donor vector previously rescued mice with GSD Ia when delivered as an AAV8 vector, reversing hypoglycemia and expressing 25% of normal G6Pase activity in the liver.[3] Puppies treated with genome editing also had a stably integrated G6PC transgene for at least 16 months, and both

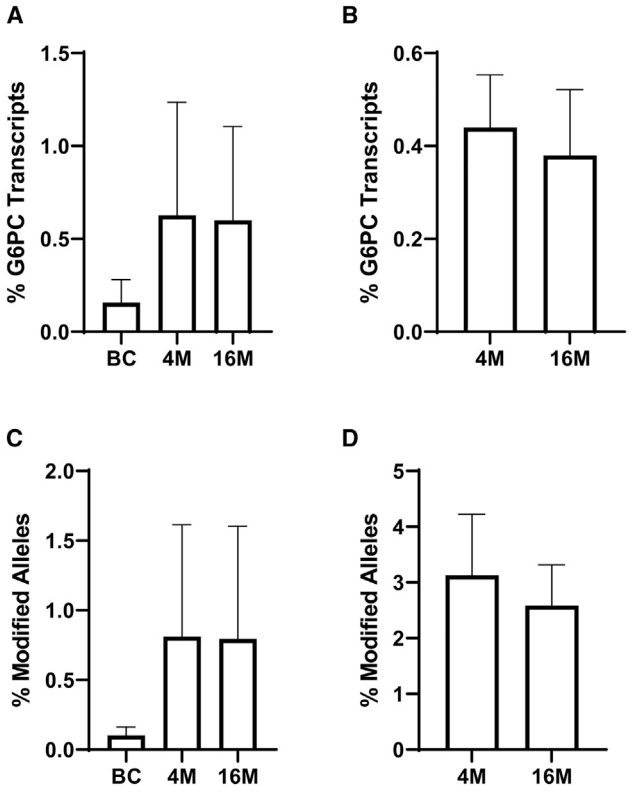

Figure 6. Integrated transgene expression and indel formation at the dog G6PC locus

(A) Dog and (B) puppy mRNA was extracted and converted to cDNA. Next-generation sequencing was performed to determine the percentage of canine G6PC transcripts expressed from the integrated cG6PC transgene. CRISPR-Cas9 activity was measured by detecting indels generated at the G6PC locus in dogs. The target region of the G6PC locus was amplified by PCR followed by next-generation sequencing of the amplicon. (C) The percentage of modified G6PC alleles is quantified by the amount of indels in dogs and (D) puppies treated with genome editing vectors. Mean ± standard deviation is shown.

adult dog and puppy groups had stably decreased liver glycogen after combined treatment with gene therapy and genome editing. Editing efficacy was less than 1%, indicating the need to increase the efficiency of HDR to achieve long-term, stand-alone treatment with genome editing. This need is emphasized by a multi-year follow-up study of AAV vector-mediated gene therapy in dogs with GSD Ia that showed that expression of up to 28% of normal G6Pase activity in liver failed to prevent HCA and HCC formation in absence of intensive nutritional support.[27,28] However, the threshold for efficacious therapy might be lower in mice with GSD Ia, given that a study of gene therapy in the mouse model confirmed that only 3% of normal G6Pase activity was sufficient to prevent tumor formation for 70–90 weeks.[4]

The inclusion of long homology arms in the donor vector complicated efforts to quantify the rate of HDR in this study. However, we were able to quantify HDR in all five dogs with GSD Ia after vector administration to either neonates or middle-aged adults (Figure 5). This result differs from an earlier study in which HDR-mediated editing was effective in neonatal mice with ornithine transcarbamylase deficiency, but not in adults.[10]

Limitations of this study included the small number of treated animals, which led to low power to detect benefits related to genome editing. Furthermore, the severity of GSD Ia in dogs dictated a vector design where unintegrated, episomal donor vector expressed G6Pase and corrected the underlying enzyme deficiency, which prevented the detection of additional benefits from the integration of the donor transgene. Last, our data suggest the HDR-driven incorporation of our donor transgene depends on CRISPR-Cas9-induced nuclease activity. However, we cannot rule out nuclease-independent integration or spontaneous integration of AAV. Previous studies have shown 0.5%–1% HDR both with and without nucleases.[22,23,29] AAV can spontaneously integrate into the genome and double-stranded breaks, but is reported to occur in less than 0.1% of cells.[30,31] The combination of our *in vitro* and *in vivo* experiments shows repair rates higher than that of AAV integration and suggests a benefit from nuclease activity.

This study was not designed to demonstrate safety in a formal way. Monitoring for the effects of GSD Ia confirmed that abnormalities observed were consistent with GSD Ia and not with additional toxicity from SaCas9.[27] While the treated dogs remained generally healthy without overt signs of toxicity from SaCas9 activity, a pre-existing immune response in the form of anti-SaCas9 antibodies was detected in older dogs before administration of the vector containing SaCas9, which could represent an obstacle to genome editing in humans due to pre-existing immune responses against SaCas9.[21]

Screening of potential sites for off-target activity *in vitro* did not reveal the presences of indels that reflect NHEJ following cutting with SaCas9. However, the presence of indels in cultured dog cells at the target site along with the detection of SaCas9 protein confirmed the activity of the SaCas9 transgene. *In vivo*, all five dogs contained indels at the target site in the *G6PC* gene. When we screened 10 potential off-target sites for indels caused by NHEJ, only 1 site had slightly increased indels compared with an untreated control dog (Table 1). Overall, the lack of off-target cutting *in vitro* and the low frequency of indels at the target site *in vivo* reflected a relatively low risk for genotoxicity from double-stranded DNA breaks arising from genome editing.

Overall, genome editing with AAV vectors designed to deliver the smaller SaCas9 protein as a strategy to integrate a therapeutic transgene demonstrated feasibility for GSD Ia, despite pre-existing anti-SaCas9 immunity that might have decreased transgene integration. These data support the further development of genome editing for GSD Ia and other inherited metabolic disorders involving the liver.

METHODS

Animal use

GSD Ia-affected dogs were treated with AAV vectors as described above. All dogs were maintained on diets formulated for the growth

Table 1. Off target CRISPR-Cas9 activity detection[a]

Gene	gRNA location	gRNA target sequence	PAM	Dog 3 indel %	Puppy 1 indel %	Control indel %	Genomic location
G6PC	Intron	GATGGTCAGACATTTCCAGA	GAGAAT	0.712	3.900	0.057	9:20143274-20143299
U6-ENSCAFG00000007798	Intergenic	AATGGTCAGACATTTCCAAA	GTGGAG	0.024	0.032	0.025	25:22315002-22315027
ST6GAL1[b]	Intron	AATGGTGAGAGATTTCCAGA	GAGAGA	20.500	21.200	20.600	34:19506977-19507002
C1orf95	Intron	GATGCTCAGACATTTCAAAA	CAGAAT	0.064	0.098	0.096	7:38396252-38396277
RSPRY1	Intron	AATGTTTAGACATTTCCAGA	TAGGAG	0.098	0.145	0.119	2:59172272-59172297
ZNF536	Intron	GATGGGCTGGCATTTCCAGA	ACGGGG	0.604	0.572	0.546	1:121194596-121194621
FANCC	Intron	GAGTGTCAGACACTTCCAGA	GAGAAA	0.133	0.127	0.109	1:71473173-71473198
CCDC170	Exon	GATGGTCATAAATTTCCTGA	CAGGGT	1.120	1.790	0.625	1:41875925-41875950
TG	Intron	TATAGTCAGACTTTTCCAGA	AGGAGG	0.129	0.118	0.124	13:29383324-29383349
DIXDC1	Intron	GATTTTCAGACATTTCCACA	ATGAAT	0.096	0.062	0.088	5:21154057-21154082
Pak7[B]	Exon	CATGGTGAGACATTTCCAGT	TTGGGG	46.600	46.700	47.700	24:12671044-12671069

[a]To measure off target nuclease activity by the CRISPR-Cas9 vector, 10 sites in the genome were analyzed for indel formation. The software CRISPOR was used to determine the 10 most likely off target sites based on the gRNA used in the AAV-CRISPR-Cas9 vector targeting the canine G6PC locus. Columns 1 and 2 contain the gene names and locations within the gene where the gRNA targets. Columns 3 and 4 contain the target sequence and adjacent PAM for each site analyzed and differences with the G6PC target sequence (row 3). Column 8 contains the genomic location of the next-generation sequencing of amplicons. All 10 off-target sites were analyzed for the adult dog and puppy that had the highest on target indel formation and transgene integration (dog 3 and puppy 1) and an untreated control dog. The percentage of indels for each site is shown in columns 5–7. The percentage of indels was equal for the treated dogs compared with the control and typically less than 1%. Next-generation sequencing did reveal some natural genetic variation in the dog genome as the high rates of indels is ST6GAL1 and PAK7 is likely not due to CRISPR-Cas9.

[b]Next-generation sequencing did reveal natural genetic variation in the dog genome as the high rates of indels in ST6GAL1 and PAK7 are likely not due to CRISPR-Cas9, because it was detected in the control.

and stage of each dog. Occasionally, appetite was suppressed in the dogs, requiring a variety of dog food options available throughout each dog's life. In general, most dogs were able to thrive on 2–3 feedings per day, similar to unaffected dogs. However, in the first months puppies developed recurrent hypoglycemia that was managed by vector re-administration as described.[20] For re-administration, AAV vectors were pseudo-typed as a new serotype to avoid the neutralizing effects of anti-AAV antibodies. This study was approved by the Duke Institutional Animal Care and Use Committee.

Fibroblast transfection and analysis

Primary canine fibroblasts were transfected with SaCas9 and cG6PC plasmids using Lipofectamine 3000 (Thermo Fisher Scientific, Waltham, MA; #L3000015) according to manufacturer's protocol. Donor vector integration and indels were quantified as described below.

AAV production and administration

AAV serotypes have been described.[32] The AAV vector plasmid pAAV-Cas9 contained the vector gene comprised of a terminal repeat (TR) at each end flanking two transgenes: (1) the U6 promoter expressing a gRNA and (2) a minimal cytomegalovirus promoter expressing Cas9 from *S. aureus*[26] with an FLAG tag and bovine growth hormone genomic polyadenylation sequence. The second AAV vector plasmid, pAAV-G6Pase, contained a TR at each end flanking the transgene consisting of the canine G6Pc cDNA. The cDNA was flanked upstream by the 5′ untranslated region (UTR) genomic sequence of canine *G6PC*, including a 1361-bp canine *G6PC* promoter.[3] Downstream of the cDNA is the human growth hormone genomic polyadenylation sequence followed by the intron 1 genomic sequence of canine *G6PC*. The vector AAV-G6Pase encoding human G6Pase was used for gene therapy and has been described.[5] Vectors were purified and quantified by Southern blot as described.[20]

Detection of DNA integration

Fibroblast and liver DNA were extracted using the Wizard Genomic DNA Purification Kit (Promega, Madison, WI, USA). The canine G6Pc locus was amplified by Q5 Taq Polymerase (NEB, Ipswich, MA, USA) with the following reagents: 5 μL Q5 buffer, 5 μL high GC enhancer solution, 2 μL 2.5 mM dNTP mix, 1.25 μL 10 μM primer P1 (5′-GCCAGACAAGAAGTCTTTGTAAGGC-3′), 1.25 μL 10 μM primer P4 (5′-GCTGTTGAATAGGGGACATTACAGACG-3′), 9.25 μL water, 1 μL (100 ng) genomic DNA, and 0.25 μL Q5 Taq Polymerase. Cycling conditions were 35 cycles of denaturation at 95°C for 30 s, annealing at 59°C for 30 s, extension at 72°C for 2 min, followed by incubation at 4°C. One microliter of first-round PCR products was used in a nested reaction with the same conditions except primers were P2 (5′-GGACATGGACAAGGTCGAGACATTCC-3′) and P3 (5′-CCAAAGAATATTAGAGCTAGAAG-3′) and cycling was 30 cycles. Control primers were P5 (5′-CGTCTGTAATGTCCCC TATTCAACAGC-3′) and P6 (5′-AAGTACCTAGAACAGTGTCTG GCACAG-3′).

Western blotting

Fibroblasts from cell culture and dog liver tissue samples were homogenized in radioimmunoprecipitation assay lysis buffer (Thermo Fisher Scientific), and protein concentration was determined via BCA Assay (Thermo Fisher Scientific). Laemmli sample buffer was added (250 mM/L Tris [pH 7.4], 2% w/v SDS, 25% v/v glycerol, 10% v/v 2-mercaptoethanol, 0.01% w/v bromophenol blue), and gel samples were boiled for 10 min and stored at −20°C until

SDS-PAGE was performed. Samples were run on an SDS-polyacrylamide gel and transferred to a polyvinylidene difluoride membrane (Bio-Rad Laboratories, Hercules, CA). Washing, blocking, and antibody solutions were prepared in PBS with 0.1% Tween 20. After washing, membranes were blocked for an hour in 5% skim milk, incubated overnight at 4°C with the primary antibody (Santa Cruz HA-Tag Antibody #sc-7392), washed, and re-incubated for an hour with the secondary antibody (Sigma Chemical Co., St. Louis, MO, mouse-HRP #12-249). After a final wash, enhanced chemiluminescence detection reagents (Thermo Fisher Scientific) were added to the membrane, and protein signal was read using a ChemiDoc imaging system (Bio-Rad Laboratories). Membranes were also imaged for β-actin control signal after stripping and re-blocking the membrane.

Quantification of vector DNA

AAV vector genome copy number was measured by quantitative real-time PCR with liver genomic DNA and normalized to β-actin. Plasmid DNA corresponding to 0.01 to 100 copies of canine G6Pase gene (in 500 ng genomic DNA) was used in a standard curve. Quantitative PCR was performed on a Lightcycler 480 (Roche Diagnostics, Basel, Switzerland) using SYBR Green mix (Thermo Fisher Scientific) and the following primers: cG6Pc Fwd (5′-TCTTCGAC CAGCCAGACAAG-3′), cG6Pc Rev (5′-GGTCCTTTAGGAGGTCA TAG-3′), hG6PC Fwd (5′-GCAGTTCCCTGTAACCTGTGAG-3′), hG6PC Rev (5′-GGTCGGCTTTATCTTTCCCTG-3′), saCas9 Fwd (5′-GTTGGTATACACGGTGTGCCTG-3′), saCas9 Rev (5′-CTGAC GCCAGCGTCAATCAC-3′), cB-actin Fwd (5′-ATGGAATCCTGC GGCATCCATG-3′), and cB-actin Rev(5′-CAGGGTACATGGTGG TTCCAC-3′). Cycling conditions were 95°C for 5 min, followed by 45 cycles of 95°C for 10 s, 60°C for 10 s, and 72°C for 20 s followed by acquisition.

Biochemical analysis

Enzyme analysis was performed as described.[3] Briefly, tissues were flash frozen and stored at −70°C. Glycogen content was measured by complete digestion of polysaccharide using amyloglucosidase (Sigma Chemical Co.). The structure of the polysaccharide was inferred by using phosphorylase free of the debranching enzyme to measure the yield of glucose-1- phosphate. Specific G6Pase activity was measured by using glucose-6-phosphate as substrate after subtraction of nonspecific phosphatase activity as estimated by β-glycerophosphate.

Fasting study

Glucose curves for monitoring hypoglycemia were performed by fasting the dogs for up to 8 h and monitoring blood glucose every 2 h. If blood glucose dropped below 50–60 mg/dL or clinical signs of hypoglycemia occurred, the curve was stopped, and dogs were given dextrose therapy as needed and fed. Blood glucose was measured by a point of care glucometer, either the AlphaTRAK or AlphaTRAK2 (Zoetis, Parsippany, NJ).

ELISA

MAxisorp 96-well plates (Thermo Fisher Scientific) were coated with Cap7 or SasCas9 protein in carbonate buffer at 4°C overnight. A standard curve of IgG isotype (Sigma Chemical Co.) was coated to the wells in seven 2-fold dilution starting from 1 μg/mL. After blocking, plasma samples diluted at 1:100 were added to plates and incubated for 1 h at 37°C. Isotype-specific secondary antibodies coupled to horseradish peroxidase were used for detection (Southern Biotech, Birmingham, AL). Then 3,3′,5,5′-tetramethylbenzidine substrate (BD Biosciences, San Jose, CA) was added to the wells and color development was measures at 450 and 570 nm (for background subtraction) on an Enspire plate reader (PerkinElmer, Waltham, MA) after blocking the reaction with H_2SO_4.

Quantification of nuclease activity

Using purified DNA, the canine G6PC locus was amplified using one round of PCR following the conditions mentioned above except for the primers dogsurveyorFwd (5′-GCCTTCTATGTCCTCTTT CCC-3′) and dogsurveyorRev (5′-TTAGAGCCCAGTTCTCTGGG TTAC-3′). The PCR product was analyzed using the Surveyor Mutation Detection Kit (Integrated DNA Technologies, Coralville, IA) according to manufacturers instructions. The PCR products were also sequenced using Sanger sequencing methods (Eton Biosciences, Durham, NC).

DNA integration quantification

A synthetic DNA fragment was generated by PCR with primers P1 and P4 in the first round of PCR, followed by primers P2 and P3 using the integration PCR conditions detailed above, which contained the junction fragment from the 3′ end of the canine *G6PC* cDNA in the transgene to the intron 1 *G6PC* sequence in dog genomic DNA. Serial dilutions of the synthetic DNA templates were made and used as the starting template for each PCR reaction to generate the standard curve. Dog genomic DNA was amplified simultaneously to measure the level of integrated transgene and the *G6PC* locus.[23]

Transcript analysis

RNA was isolated from dog liver biopsies and converted to cDNA using RevertAid First Strand cDNA Synthesis Kit (Thermo Fisher Scientific). G6PC transcripts were amplified by PCR using a forward primer in the 5′ UTR (5′-TGATAGCAGAGCAATCGCCAA GTC-3′) and the reverse primer in exon 2 (5′-AGGGTAGATGT GACCATCACGTAG-3′). The PCR products were purified with the Qiagen PCR Purification Kit (Qiagen, Germantown, MD, #28104). The DNA was sequenced using Illumina Mi-Seq and analyzed (performed by Azenta Lifesciences, South Plainfield, NJ). The donor AAV vector contains an BamHI restriction site −5 to −10 bp upstream of the transcription start site and the wild-type base at position 363 that is mutated in GSD Ia dogs. Transcripts without the BamHI site but with the correction at position 363 were considered to be expressed off the integration transgene and quantified with a ChemiDoc imaging system (Bio-Rad Laboratories).

Off-target indel quantification in vivo

The software CRISPOR was used to determine potential off target sites. Those sites were amplified using gene specific primers (Table S2). PCR products were purified with the Qiagen PCR Purification

Kit (#28104). The DNA was sequenced using Illumina Mi-Seq and analyzed (performed by Azenta Lifesciences).

Statistic analyses

Statistical analysis was performed using GraphPad Prism 6. Statistical significance was determined by one-way ANOVA with Tukey's multiple comparisons test. The statistical significance of comparisons is indicated as follows: *=p<0.05, **=p<0.01, ***=p<0.001, ****=p<0.0001.

DATA AVAILABILITY

Data from this study will be made available upon request.

SUPPLEMENTAL INFORMATION

Supplemental information can be found online at https://doi.org/10.1016/j.omtm.2023.03.001.

ACKNOWLEDGMENTS

The authors also would like to acknowledge technical support from Ms. Songtao Li. We would also like to acknowledge inspiration and support from Dr. Emory and Mrs. Mary Chapman and their son Christopher, and from Dr. John and Mrs. Michelle Kelly. We deeply appreciate the dedication shown by the staff of the Duke Department of Laboratory Animal Resources, as well as undergraduate students at Duke University. This work was supported by grants R01DK105434 and R56DK105434 from the National Institute of Diabetes and Digestive and Kidney Diseases; and by the resources of the Alice and Y. T. Chen Center for Genetics and Genomics. HRK was funded by a Pfizer NC Biotechnology Gene Therapy Fellowship, Agreement Number GTF-A-4026.

AUTHOR CONTRIBUTIONS

B.A. performed experiments, analyzed data, and wrote the paper. H.R.K. performed experiments and analyzed data. E.D.B. provided veterinary care, performed experiments, analyzed data, and edited the paper. D.G. performed experiments and analyzed data. E.I. performed experiments and analyzed data. D.C. provided technical advice and editing the paper. J.I.E. provided analysis of histology of dog biopsies. B.R.C. provided technical advice, shared plasmids for construction of the CRISPR-Cas9 vector, and edited the paper. D.D.K. performed experiments, analyzed data, and wrote and edited the paper.

DECLARATION OF INTERESTS

D.D.K., H.R.K., B.A., and B.R.C. have developed the technology that is being used in the study. If the technology is commercially successful in the future, the developers and Duke University may benefit financially. D.D.K. has received research/grant support from Sangamo Therapeutics, Inc. in the past.

REFERENCES

1. Koeberl, D.D., Kishnani, P.S., Bali, D., and Chen, Y.T. (2009). Emerging therapies for glycogen storage disease type I. Trends Endocrinol. Metabol. *20*, 252–258.
2. Kishnani, P.S., Austin, S.L., Abdenur, J.E., Arn, P., Bali, D.S., Boney, A., Chung, W.K., Dagli, A.I., Dale, D., Koeberl, D., et al. (2014). Diagnosis and management of glycogen storage disease type I: a practice guideline of the American College of Medical Genetics and Genomics. Genet. Med. *16*, e1.
3. Koeberl, D.D., Sun, B.D., Damodaran, T.V., Brown, T., Millington, D.S., Benjamin, D.K., Jr., Bird, A., Schneider, A., Hillman, S., Jackson, M., et al. (2006). Early, sustained efficacy of adeno-associated virus vector-mediated gene therapy in glycogen storage disease type Ia. Gene Ther. *13*, 1281–1289.
4. Lee, Y.M., Jun, H.S., Pan, C.J., Lin, S.R., Wilson, L.H., Mansfield, B.C., and Chou, J.Y. (2012). Prevention of hepatocellular adenoma and correction of metabolic abnormalities in murine glycogen storage disease type Ia by gene therapy. Hepatology *56*, 1719–1729.
5. Luo, X., Hall, G., Li, S., Bird, A., Lavin, P.J., Winn, M.P., Kemper, A.R., Brown, T.T., and Koeberl, D.D. (2011). Hepatorenal correction in murine glycogen storage disease type I with a double-stranded adeno-associated virus vector. Mol. Ther. *19*, 1961–1970.
6. Cunningham, S.C., Spinoulas, A., Carpenter, K.H., Wilcken, B., Kuchel, P.W., and Alexander, I.E. (2009). AAV2/8-mediated correction of OTC deficiency is robust in adult but not neonatal Spf(ash) mice. Mol. Ther. *17*, 1340–1346.
7. Cotugno, G., Annunziata, P., Tessitore, A., O'Malley, T., Capalbo, A., Faella, A., Bartolomeo, R., O'Donnell, P., Wang, P., Russo, F., et al. (2011). Long-term amelioration of feline Mucopolysaccharidosis VI after AAV-mediated liver gene transfer. Mol. Ther. *19*, 461–469.
8. Lee, E.K., Hu, C., Bhargava, R., Rozengurt, N., Stout, D., Grody, W.W., Cederbaum, S.D., and Lipshutz, G.S. (2012). Long-term survival of the juvenile lethal arginase-deficient mouse with AAV gene therapy. Mol. Ther. *20*, 1844–1851.
9. Gautam, S., Zhang, L., Arnaoutova, I., Lee, C., Mansfield, B.C., and Chou, J.Y. (2020). The signaling pathways implicated in impairment of hepatic autophagy in glycogen storage disease type Ia. Hum. Mol. Genet. *29*, 834–844.
10. Landau, D.J., Brooks, E.D., Perez-Pinera, P., Amarasekara, H., Mefferd, A., Li, S., Bird, A., Gersbach, C.A., and Koeberl, D.D. (2016). In vivo zinc finger nuclease-mediated targeted integration of a glucose-6-phosphatase transgene promotes survival in mice with glycogen storage disease type Ia. Mol. Ther. *24*, 697–706.
11. Yang, Y., Wang, L., Bell, P., McMenamin, D., He, Z., White, J., Yu, H., Xu, C., Morizono, H., Musunuru, K., et al. (2016). A dual AAV system enables the Cas9-mediated correction of a metabolic liver disease in newborn mice. Nat. Biotechnol. *34*, 334–338.
12. Arnaoutova, I., Zhang, L., Chen, H.D., Mansfield, B.C., and Chou, J.Y. (2021). Correction of metabolic abnormalities in a mouse model of glycogen storage disease type Ia by CRISPR/Cas9-based gene editing. Mol. Ther. *29*, 1602–1610.
13. Schmidt, F., and Grimm, D. (2015). CRISPR genome engineering and viral gene delivery: a case of mutual attraction. Biotechnol. J. *10*, 258–272.
14. Nelson, C.E., Hakim, C.H., Ousterout, D.G., Thakore, P.I., Moreb, E.A., Castellanos Rivera, R.M., Madhavan, S., Pan, X., Ran, F.A., Yan, W.X., et al. (2016). In vivo genome editing improves muscle function in a mouse model of Duchenne muscular dystrophy. Science *351*, 403–407.
15. Long, C., Amoasii, L., Mireault, A.A., McAnally, J.R., Li, H., Sanchez-Ortiz, E., Bhattacharyya, S., Shelton, J.M., Bassel-Duby, R., and Olson, E.N. (2016). Postnatal genome editing partially restores dystrophin expression in a mouse model of muscular dystrophy. Science *351*, 400–403.
16. Friedland, A.E., Baral, R., Singhal, P., Loveluck, K., Shen, S., Sanchez, M., Marco, E., Gotta, G.M., Maeder, M.L., Kennedy, E.M., et al. (2015). Characterization of Staphylococcus aureus Cas9: a smaller Cas9 for all-in-one adeno-associated virus delivery and paired nickase applications. Genome Biol. *16*, 257.
17. Farah, B.L., Landau, D.J., Wu, Y., Sinha, R.A., Loh, A., Bay, B.H., Koeberl, D.D., and Yen, P.M. (2017). Renal endoplasmic reticulum stress is coupled to impaired autophagy in a mouse model of GSD Ia. Mol. Genet. Metabol. *122*, 95–98.
18. Farah, B.L., Landau, D.J., Sinha, R.A., Brooks, E.D., Wu, Y., Fung, S.Y.S., Tanaka, T., Hirayama, M., Bay, B.H., Koeberl, D.D., and Yen, P.M. (2016). Induction of autophagy improves hepatic lipid metabolism in glucose-6-phosphatase deficiency. J. Hepatol. *64*, 370–379.
19. Koeberl, D.D., Pinto, C., Sun, B., Li, S., Kozink, D.M., Benjamin, D.K., Jr., Demaster, A.K., Kruse, M.A., Vaughn, V., Hillman, S., et al. (2008). AAV vector-mediated

reversal of hypoglycemia in canine and murine glycogen storage disease type Ia. Mol. Ther. *16*, 665–672.

20. Demaster, A., Luo, X., Curtis, S., Williams, K.D., Landau, D.J., Drake, E.J., Kozink, D.M., Bird, A., Crane, B., Sun, F., et al. (2012). Long-term efficacy following readministration of an adeno-associated virus vector in dogs with glycogen storage disease type Ia. Hum. Gene Ther. *23*, 407–418.
21. Charlesworth, C.T., Deshpande, P.S., Dever, D.P., Camarena, J., Lemgart, V.T., Cromer, M.K., Vakulskas, C.A., Collingwood, M.A., Zhang, L., Bode, N.M., et al. (2019). Identification of preexisting adaptive immunity to Cas9 proteins in humans. Nat. Med. *25*, 249–254.
22. Porro, F., Bortolussi, G., Barzel, A., De Caneva, A., Iaconcig, A., Vodret, S., Zentilin, L., Kay, M.A., and Muro, A.F. (2017). Promoterless gene targeting without nucleases rescues lethality of a Crigler-Najjar syndrome mouse model. EMBO Mol. Med. *9*, 1346–1355.
23. Chandler, R.J., Venturoni, L.E., Liao, J., Hubbard, B.T., Schneller, J.L., Hoffmann, V., Gordo, S., Zang, S., Ko, C.W., Chau, N., et al. (2021). Promoterless, nuclease-free genome editing confers a growth advantage for corrected hepatocytes in mice with methylmalonic acidemia. Hepatology *73*, 2223–2237.
24. Richards, D.Y., Winn, S.R., Dudley, S., Nygaard, S., Mighell, T.L., Grompe, M., and Harding, C.O. (2020). AAV-mediated CRISPR/CAS9 gene editing in murine phenylketonuria. Mol. Ther. Methods Clin. Dev. *17*, 234–245.
25. Yin, H., Xue, W., Chen, S., Bogorad, R.L., Benedetti, E., Grompe, M., Koteliansky, V., Sharp, P.A., Jacks, T., and Anderson, D.G. (2014). Genome editing with Cas9 in adult mice corrects a disease mutation and phenotype. Nat. Biotechnol. *32*, 551–553.
26. Trinh, K.Y., O'Doherty, R.M., Anderson, P., Lange, A.J., and Newgard, C.B. (1998). Perturbation of fuel homeostasis caused by overexpression of the glucose-6-phosphatase catalytic subunit in liver of normal rats. J. Biol. Chem. *273*, 31615–31620.
27. Brooks, E.D., Landau, D.J., Everitt, J.I., Brown, T.T., Grady, K.M., Waskowicz, L., Bass, C.R., D'Angelo, J., Asfaw, Y.G., Williams, K., et al. (2018). Long-term complications of glycogen storage disease type Ia in the canine model treated with gene replacement therapy. J. Inherit. Metab. Dis. *41*, 965–976.
28. Brooks, E.D., Kishnani, P.S., and Koeberl, D.D. (2018). Letter to the Editors: concerning "Long-term safety and efficacy of AAV gene therapy in the canine model of glycogen storage disease type Ia" by Lee et al. J. Inherit. Metab. Dis. *41*, 913–914.
29. Barzel, A., Paulk, N.K., Shi, Y., Huang, Y., Chu, K., Zhang, F., Valdmanis, P.N., Spector, L.P., Porteus, M.H., Gaensler, K.M., and Kay, M.A. (2015). Promoterless gene targeting without nucleases ameliorates haemophilia B in mice. Nature *517*, 360–364.
30. Deyle, D.R., and Russell, D.W. (2009). Adeno-associated virus vector integration. Curr. Opin. Mol. Therapeut. *11*, 442–447.
31. Sabatino, D.E., Bushman, F.D., Chandler, R.J., Crystal, R.G., Davidson, B.L., Dolmetsch, R., Eggan, K.C., Gao, G., Gil-Farina, I., Kay, M.A., et al. (2022). Evaluating the state of the science for adeno-associated virus integration: an integrated perspective. Mol. Ther. *30*, 2646–2663.
32. Gao, G.P., Alvira, M.R., Wang, L., Calcedo, R., Johnston, J., and Wilson, J.M. (2002). Novel adeno-associated viruses from rhesus monkeys as vectors for human gene therapy. Proc. Natl. Acad. Sci. USA *99*, 11854–11859.

OMTM, Volume *29*

Supplemental information

Genome editing using *Staphylococcus aureus* Cas9 in a canine model of glycogen storage disease Ia

Benjamin Arnson, Hye Ri Kang, Elizabeth D. Brooks, Dorothy Gheorghiu, Ekaterina Ilich, David Courtney, Jeffrey I. Everitt, Bryan R. Cullen, and Dwight D. Koeberl

Table S1: GSD Ia dog vector and medication treatment.

Dog	Sex	Age when vector/medication administered	AAV vector/medication	Vector/Medication Dose
Dog 1	M	1 day	AAV2/9 G6Pase	$2x10^{13}$ vp/kg
		2 months	AAV2/10 G6Pase	5×10^{12} vp/kg
		2-3 months	Resveratrol	5 mg/kg/day
		3 months	AAV2/8 G6Pase	2×10^{13} vp/kg
		29-32 months	Bezafibrate[A]	4 mg/kg/day
		34 months	AAV2/7 G6Pase + AAV2/7 CRISPR	1×10^{13} vp/kg + 2×10^{12} vp/kg
Dog 2	M	1 day	AAV2/9 G6Pase	2×10^{13} vp/kg
		2 months	AAV2/10 G6Pase	5×10^{12} vp/kg
		2-3 months	Resveratrol	5 mg/kg/day
		3 months	AAV2/8 G6Pase	7×10^{12} vp/kg
		29-32 months	Bezafibrate[A]	4 mg/kg/day
		34 months	AAV2/7 G6Pase + AAV2/7 CRISPR	1×10^{13} vp/kg + 2×10^{12} vp/kg
Dog 3	M	1 day	AAV2/9 G6Pase	2×10^{13} vp/kg
		2 months	AAV2/10 G6Pase	5×10^{12} vp/kg
		2-3 months	Resveratrol	5 mg/kg/day
		3 months	AAV2/8 G6Pase	2×10^{12} vp/kg
		30-32 months	Bezafibrate[A]	4 mg/kg/day
		34 months	AAV2/7 G6Pase + AAV2/7 CRISPR	1×10^{13} vp/kg + 2×10^{12} vp/kg
Puppy 1	M	2 days	AAV2/7 G6Pase + AAV2/7 CRISPR	4×10^{13} vp/kg + 8×10^{12} vp/kg
		2 months	AAV2/10 G6Pase	3×10^{12} vp/kg
		3 months	AAV2/8 G6Pase	1×10^{13} vp/kg
		12-16 months	Bezafibrate[A]	4 mg/kg/day
Puppy 2	M	2 days	AAV2/7 G6Pase + AAV2/7 CRISPR	5×10^{13} vp/kg + 1×10^{13} vp/kg
		2 months	AAV2/9 G6Pase	3×10^{13} vp/kg

[A]Resveratrol was administered to stimulate autophagy as described.[1]
[B]Description and results of bezafibrate treatment described.[2]

Table S2: Off target CRISPR/Cas9 primers: Gene names, genomic locations, and primers used to generate PCR products for next generation sequencing of amplicons, based on the reference genome.[3]

Gene	Genomic Location	Fwd Primer	Rev Primer
G6PC	9:20143274-20143299	TGTCCGTGATTGCAGACCTCAG	AGATGATCCAGAGTCAGGAGGG
U6-ENSCAFG00000007798	25:22315002-22315027	CTGTTCGAAGAGTCTGCATGTAAG	GAGGGGTTTTAGGAAGTGCTGG
ST6GAL1	34:19506977-19507002	CAGCTTGTTCACAACCAGACTC	CAGTTTTCTCCAGGCTCCTAAC
C1orf95	7:38396252-38396277	TGGGACATTTTAGGGAGCCAAG	CATTCTCGTCTTGGAACGTGTG
RSPRY1	2:59172272-59172297	GCAAGATAAGAGTCGGTCTTCGTG	ACACTAGCAGTCATACGGACTC
ZNF536	1:121194596-121194621	ACTGGGGCTCGTATCTCGG	CAAGGGAGAGGCTTCAGAATCG
FANCC	1:71473173-71473198	TACAGGGAGCCTGCTTCTGCC	CACAATCCCTTGTGGGAAGGGC
CCDC170	1:41875925-41875950	AGCACATCATTCATTCCTGGGC	CCAGTTCACTTCGAGCGTCTTC
TG	13:29383324-29383349	GCATCCCTGGGATCCTTAGG	TAGCTGAGCGTGAGAAGGGG
DIXDC1	5:21154057-21154082	CTGTTTAGCTGGCATTGACTCC	GCTTTTGTCTGGTGTCATCCCC
Pak7	24:12671044-12671069	CTCTGGAAGAGCTACATAGTCATC	GTACCATGAACTTTTAGGACGGTC

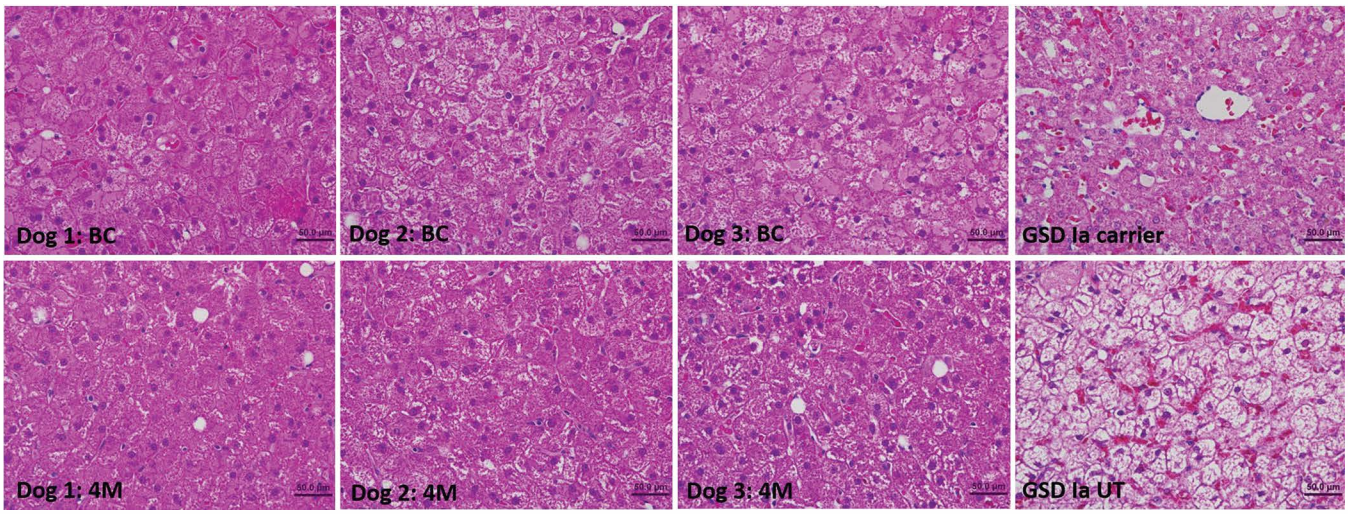

Figure S1: GSD Ia dog liver before and after genome editing. Photomicrographs of hepatic sections of Dogs 1-3 pre-treatment (BC) reveal mosaic pattern of diffuse hepatocyte hypertrophy with vacuolar and glycogen changes and inconspicuous hepatic sinusoids relative to that of the GSD-Ia carrier liver. There is minimal (Dog 2) to mild (Dog 1 and 3) glycogen depletion noted in the post-treatment hepatic sections (4M). In comparison with an untreated adult dog (GSD Ia UT), vacuolar changes and glycogen accumulations were markedly decreased for Dogs 1-3. The photomicrograph of the liver from GSD Ia UT shows marked diffuse vacuolar change with maintenance of prominent hepatic sinusoids congested with erythrocytes. Magnification 400x.

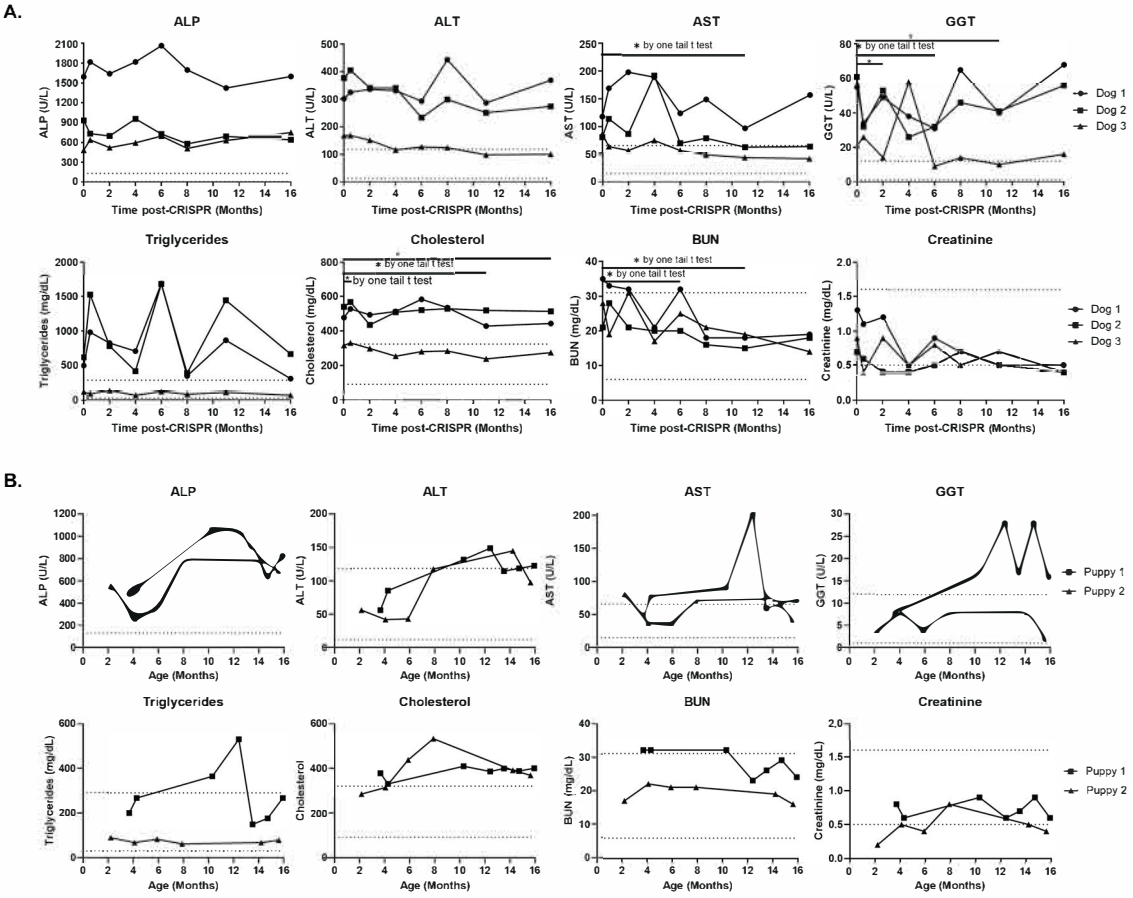

Figure S2:Oog blood chemistry. (A) Blood chemistry immediately before (T=0) and following CRISPR treatment in adult and (8) neonatal GSD Ia dogs. Dashed lines indicate normal ranges.* $p<0.05$ with Student's T test or one tail T test as indicated at each time point compared to baseline (T=0).

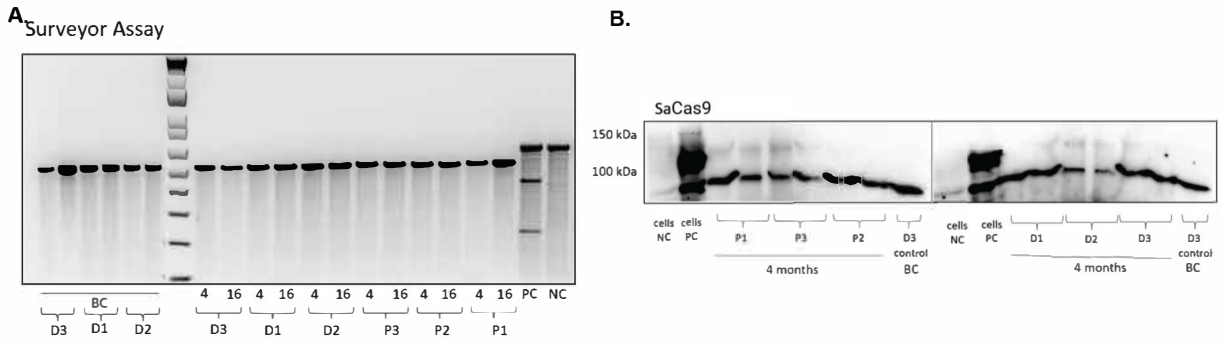

Figure S3: AAV vector administration safety and efficiency analysis. To examine the safety of gene editing Surveyor Assay was used. Positive control (PC) and negative control (NC) are indicated. (A) No on-target cleavage was detected on dog and puppy liver samples after4 and 16 months of AAV vector administration. (8) The presence of SaCas9 protein with 128 kDa size on 4 months liver samples was visualized by western blot analysis.

References

1 Ding, S., Jiang, J., Zhang, G., Bu, Y., Zhang, G. and Zhao, X. (2017). Resveratrol and caloric restriction prevent hepatic steatosis by regulating SIRT1-autophagy pathway and alleviating endoplasmic reticulum stress in high-fat diet-fed rats. PLoS One. *12*, e0183541.

2 Waskowicz, L. R., Zhou, J., Landau, D. J., Brooks, E. D., Lim, A., Yavarow, Z. A., Kudo, T., Zhang, H., Wu, Y., Grant, S. et al. (2019). Bezafibrate induces autophagy and improves hepatic lipid metabolism in glycogen storage disease type Ia. Hum Mol Genet. *28*, 143-154.

3 Canis familiaris Canfam 3.1 (*Ensembl 104: May 2021)* GRCh38.p13.